ESC European Society of Cardiology

European Heart Journal - Cardiovascular Imaging (2022) **23**, 352–362
doi:10.1093/ehjci/jeab210

ORIGINAL PAPER

Phenotyping hypertrophic cardiomyopathy using cardiac diffusion magnetic resonance imaging: the relationship between microvascular dysfunction and microstructural changes

Arka Das [1], Christopher Kelly[1], Irvin Teh[1], Christopher Nguyen[2,3,4,5], Louise A.E. Brown[1], Amrit Chowdhary [1], Nicholas Jex [1], Sharmaine Thirunavukarasu[1], Noor Sharrack [1], Miroslawa Gorecka[1], Peter P. Swoboda[1], John P. Greenwood[1], Peter Kellman [6], James C. Moon[7], Rhodri H. Davies[7], Luis R. Lopes[7,8], George Joy [7], Sven Plein[1], Jürgen E. Schneider[1], and Erica Dall'Armellina[1,*]

[1]Biomedical Imaging Science Department, Leeds Institute of Cardiovascular and Metabolic Medicine, University of Leeds, Leeds Teaching Hospitals NHS Trust, Leeds LS2 9JT, UK; [2]Cardiovascular Research Center, Massachusetts General Hospital, Charlestown, 55 Fruit St, Boston, MA 02114, USA; [3]A. A. Martinos Center for Biomedical Imaging, Massachusetts General Hospital, Charlestown, 55 Fruit St, Boston, MA 02114, USA; [4]Department of Medicine, Harvard Medical School, 25 Shattuck St, Boston, MA 02115, USA; [5]Biomedical Imaging Research Institute, Cedars-Sinai Medical Centre, 116 N Robertson Blvd, Los Angeles, CA 90048, USA; [6]National Heart, Lung, and Blood Institute, National Institutes of Health, DHHS, 31 Center Dr, Bethesda, MD 20892, USA; [7]Barts Heart Centre, The Cardiovascular Magnetic Resonance Imaging Unit and The Inherited Cardiovascular Diseases Unit, St Bartholomew's Hospital, West Smithfield, London EC1A 7BE, UK; and [8]Centre for Heart Muscle Disease, Institute of Cardiovascular Science, University College London, Gower St, London WC1E 6BT, UK

Received 23 June 2021; editorial decision 23 September 2021; accepted 16 October 2021; online publish-ahead-of-print 25 October 2021

Aims Microvascular dysfunction in hypertrophic cardiomyopathy (HCM) is predictive of clinical decline, however underlying mechanisms remain unclear. Cardiac diffusion tensor imaging (cDTI) allows *in vivo* characterization of myocardial microstructure by quantifying mean diffusivity (MD), fractional anisotropy (FA) of diffusion, and secondary eigenvector angle (E2A). In this cardiac magnetic resonance (CMR) study, we examine associations between perfusion and cDTI parameters to understand the sequence of pathophysiology and the interrelation between vascular function and underlying microstructure.

Methods and results Twenty HCM patients underwent 3.0T CMR which included: spin-echo cDTI, adenosine stress and rest perfusion mapping, cine-imaging, and late gadolinium enhancement (LGE). Ten controls underwent cDTI. Myocardial perfusion reserve (MPR), MD, FA, E2A, and wall thickness were calculated per segment and further divided into subendocardial (inner 50%) and subepicardial (outer 50%) regions. Segments with wall thickness ≤11 mm, MPR ≥2.2, and no visual LGE were classified as 'normal'. Compared to controls, 'normal' HCM segments had increased MD (1.61 ± 0.09 vs. $1.46 \pm 0.07 \times 10^{-3}$ mm^2/s, $P = 0.02$), increased E2A ($60 \pm 9°$ vs. $38 \pm 12°$, $P < 0.001$), and decreased FA (0.29 ± 0.04 vs. 0.35 ± 0.02, $P = 0.002$). Across all HCM segments, subendocardial regions had higher MD and lower MPR than subepicardial (MD_{endo} $1.61 \pm 0.08 \times 10^{-3}$ mm^2/s vs. MD_{epi} $1.56 \pm 0.18 \times 10^{-3}$ mm^2/s, $P = 0.003$, MPR_{endo} 1.85 ± 0.83, MPR_{epi} 2.28 ± 0.87, $P < 0.0001$).

*Corresponding author. Tel: +44 (01133) 438306. E-mail: e.dallarmellina@leeds.ac.uk

Conclusion In HCM patients, even in segments with normal wall thickness, normal perfusion, and no scar, diffusion is more isotropic than in controls, suggesting the presence of underlying cardiomyocyte disarray. Increased E2A suggests the myocardial sheetlets adopt hypercontracted angulation in systole. Increased MD, most notably in the subendocardium, is suggestive of regional remodelling which may explain the reduced subendocardial blood flow.

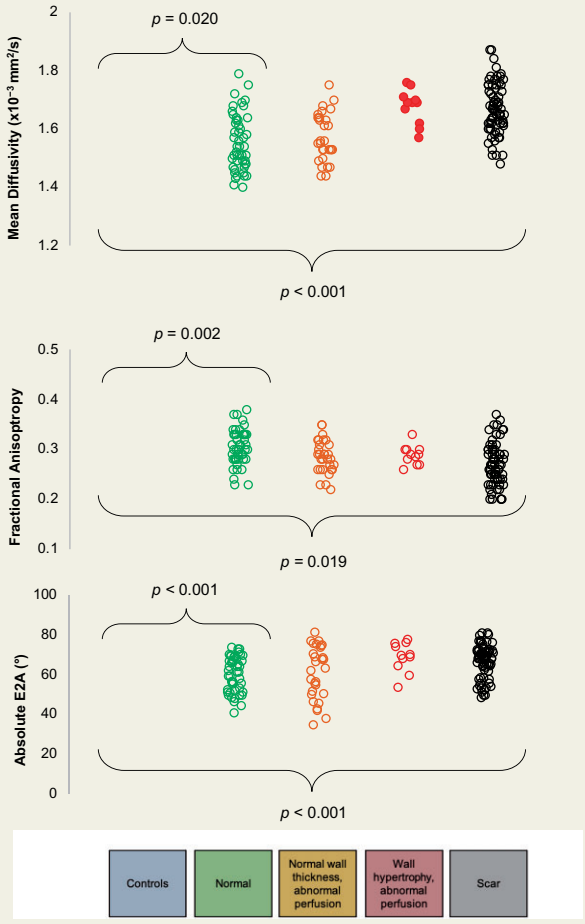

Keywords hypertrophic cardiomyopathy • microvascular dysfunction • diffusion tensor imaging

Introduction

Hypertrophic cardiomyopathy (HCM) is the most common inherited cardiac condition, characterized by unexplained myocardial hypertrophy in the absence of another cardiac or systemic disease. Genetic mutations encoding for the sarcomeric proteins which form the contractile apparatus of cardiomyocytes have been identified as a cause for the disease.[1] Histopathological changes include cardiomyocyte disarray, interstitial, and perivascular fibrosis; however, how these features develop and affect prognosis is not fully understood.[2] Microvascular dysfunction (MVD) is a common feature of HCM[3] and is thought to be responsible for ischaemia-mediated myocyte death in HCM, which ultimately leads to replacement fibrosis and left ventricular (LV) remodelling.[4] Prospective studies have identified the degree of MVD as an independent predictor of clinical decline and death in HCM patients; meanwhile, patients can remain asymptomatic with severe MVD for several years prior to deterioration.[5] Hence MVD has been recognized as a potential target for prevention of disease progression and heart failure in HCM; but effective disease-modifying therapies have proved elusive. This may in-part be because of the incomplete understanding of the pathophysiological process. Abnormal muscle, abnormal physiology, and abnormal architecture form the basis of various proposed mechanisms to explain the typical subendocardial

pattern of hyperaemic ischaemia. While the cause is thought to be multifactorial, histological studies to date have failed to demonstrate any relationship between fibre disarray, fibrosis, and small vessel disease.[6]

Cardiac diffusion tensor imaging (cDTI) is a cardiac magnetic resonance (CMR) method which allows non-invasive *in vivo* characterization of myocardial microstructure.[7,8] Mean diffusivity (MD) measures the magnitude of diffusion in a given voxel, and previous studies have shown MD to be increased in areas of interstitial fibrosis in HCM patients.[9] Fractional anisotropy (FA) measures the directional variability of diffusion in a given voxel. In the context of cardiovascular disease, FA is thought to provide a composite measure of cardiomyocyte disarray and collagen deposition; initial evidence shows that low FA values—indicating isotropic diffusion—can be predictive of adverse clinical outcomes such as ventricular arrythmia.[10,11] cDTI also enables calculation of voxel-wise helix angle (HA) and secondary eigenvector angle (E2A) maps based on the eigenvectors of the diffusion tensors. HA describes local cardiomyocyte orientation and is classically used to depict their transmurally changing arrangement,[12] while absolute E2A reflects the average orientations of laminar sheetlets.[13] At peak systole, HCM patients have higher global absolute E2A than controls, indicating their sheetlets adopt significantly steeper configurations.[13,14] Furthermore, their sheetlet mobility is impaired, so their sheetlets remain in a relatively steeper configuration in diastole than controls.[13] While cDTI studies to date have provided insights into general microstructural abnormalities, their findings are predominantly based on global difference in parameters between HCM patients and controls. In order to understand how microstructure relates to local vascular function, a more regional approach is required focussing specifically on areas with perfusion defects, such as the subendocardium. Focused analysis of myocardial segments which lack typical morphological features such as wall hypertrophy and scar may also elucidate early microstructural changes that precede clinical expression of the disease. The purpose of this study was to examine the associations between perfusion and cDTI parameters in HCM patients in order to understand the sequence of pathophysiology and the interrelation between vascular function and underlying myocardial microstructure.

Methods

Subject recruitment

HCM patients were prospectively recruited from the inherited cardiomyopathy clinic; this was inclusive of probands and relatives. The diagnosis of HCM was made independently by clinicians in keeping with current guidelines and based upon imaging including CMR, electrocardiogram, family history, and genetic testing if possible.[15] Inclusion criteria were LV wall thickness of ≥13 mm in ≥1 myocardial segment on CMR. Exclusion criteria were patients with apical HCM, the presence of any contraindication to CMR, adenosine or gadolinium-based contrast agents, systemic hypertension, significant valve disease, infiltrative cardiomyopathy, previous myocardial infarction, or coronary intervention. Healthy volunteers were enrolled from among students, staff, and alumni of the local university. They had no existing medical conditions and were not taking any regular medication. The study was conducted in accordance with the Declaration of Helsinki and was approved by the UK National Research Ethics Service (18/YH/0372, REC 39787). All participants provided written informed consent.

CMR acquisition

CMR was performed using a Prisma 3T magnetic resonance imaging (MRI) scanner (Siemens Healthineers, Erlangen, Germany). Participants were advised to avoid caffeine for 24 h before the study. The protocol for HCM patients consisted of full LV coverage by balanced steady-state free precession (bSSFP) cine data imaging and MOCO bright blood late gadolinium enhancement (LGE), three matching short-axis slices (base, mid, and apex) by cDTI, T1 mapping using a Modified Look Locker Inversion recovery (MOLLI) sequence (native 5(3)3, post-contrast 4(1)3(1)2), and stress and rest perfusion using free-breathing, motion-corrected (MOCO) automated in-line perfusion mapping.[16] The protocol for healthy controls consisted of full LV coverage with bSSFP cine-imaging and cDTI (three slices consisting of base, mid, and apex).

For perfusion imaging, adenosine was infused at a rate of 140 μg/kg/min and increased up to a maximum of 210 μg/kg/min according to haemodynamic and symptomatic response. Inadequate heart rate response was defined as <10 bpm in keeping with Society of Cardiovascular Magnetic Resonance (SCMR) guidelines.[17] An intravenous bolus of 0.05 mmol/kg gadobutrol (Gadovist, Leverkusen, Germany) was administered at 5 mL/s followed by a 20 mL saline flush using an automated injection pump (Medrad MRXperion Injection System, Bayer). This is repeated after a minimum of 10-min interval for rest perfusion acquisitions to ensure equilibration of gadolinium kinetics and that all haemodynamic effects of adenosine had resolved. Following this, a third and final bolus of 0.05 mmol/kg gadobutrol is given for acquiring LGE imaging. Blood pressure and heart rate were recorded during adenosine infusion. Perfusion mapping was performed and implemented on the scanner using the Gadgetron streaming software image reconstruction framework as previously described.[16]

cDTI acquisition

cDTI data were obtained using a second-order motion-compensated single-shot spin-echo EPI sequence as previously reported.[18,19] Data were acquired whilst free-breathing without respiratory navigation. The effects of motion were mitigated by acquisition of multiple repetitions and diffusion encoding directions. Acquisition parameters were: TE/TR 77 ms/3 R-R intervals, field of view 320 × 121 mm^2, matrix size 138 × 52, in-plane resolution 2.3 × 2.3 mm^2, 8 mm slice thickness, 8 mm inter-slice gap, and partial Fourier = 7/8. Scout diffusion-weighted (DW) data were acquired with diffusion-weighting applied in three orthogonal directions to ensure data quality. Each full data set comprised *b*-values of 100 s/mm^2 (3 DW directions, 12 repetitions), and 450 s/mm^2 (30 DW directions, 6 repetitions). Cine data were used to define the time from R peak to maximum systole. The trigger delay was defined as ∼30% of maximum systole.

CMR analysis

On cine, LGE, native T1, and post-contrast T1 images, using cvi42 software (Circle Cardiovascular Imaging, Calgary, Canada), LV subendocardial and subepicardial borders were defined by manual planimetry excluding papillary muscles at end-systole and end-diastole. LV mass, end-diastolic volumes, end-systolic volumes, and LV ejection fraction were measured from short-axis cine images. Maximal wall thickness was measured using a machine learning algorithm as previously described.[20] The LV short-axis stack of LGE images was first assessed visually for the presence of LGE, followed by quantification when LGE was present, as done in previous studies.[21] LGE was defined as areas of signal intensity ≥5 SDs from normal myocardium and was expressed both as a percentage of the segment, and the percentage of LV mass. On T1 maps, a 10% offset

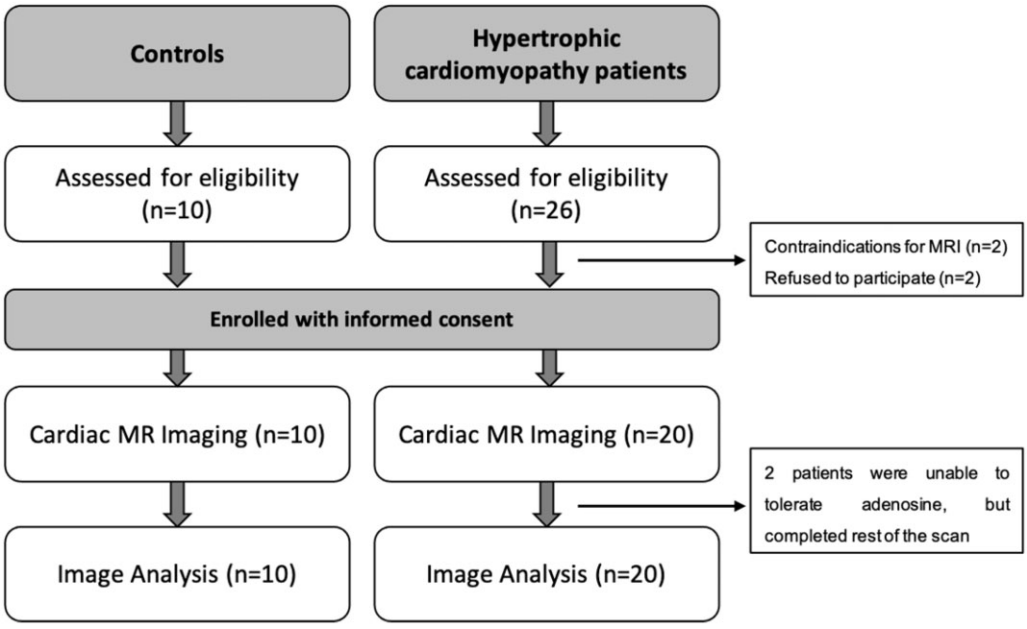

Figure 1 Flowchart of study enrolment.

Table 1 Characteristics of HCM patients and control subjects

	HCM (n = 20)	Controls (n = 10)	P-value
Age (years)	48 ± 18	27 ± 9	<0.01
Male (n)	8/20	4/10	1.00
BSA (m^2)	1.9 ± 0.2	2.2 ± 0.4	0.19
Genotype positive	5/20		
LV end-diastolic volume index (mL/m^2)	78 ± 14	80 ± 10	0.65
LV ejection fraction (%)	67 ± 6	64 ± 4	0.76
LV mass index (g/m^2)	81 ± 41	61 ± 16	0.31
Maximal LV wall thickness (mm)	19 ± 5	11 ± 1	<0.001
Left atrial diameter (mm)	43 ± 6	35 ± 2	<0.001
Presence of left ventricular outflow obstruction (n)	6/20		
Global T1 (ms)	1323 ± 75		
Global ECV (%)	27 ± 4		
LGE present (n)	17 (85%)		
LGE (% of LV mass)	5.9 ± 10.1		

Values are displayed as mean ± standard deviation for continuous variables. Departmental 3.0T scanner reference range for native T1 = 1158 ± 80 ms.
ECV, extracellular volume; HCM, hypertrophic cardiomyopathy; LGE, late gadolinium enhancement; LV, left ventricle

was applied to subendocardial and subepicardial borders to minimize partial volume effect. Extracellular volume (ECV) was calculated using the formula 'myocardial ECV = (1 - haematocrit) × ($\Delta R1_{myocardium}/\Delta R1_{blood}$), where R1 = 1/T1', with haematocrit measured from blood tests on the day of the CMR scan. Global and segmental mean blood flow (MBF) were calculated inline from the perfusion maps (where each pixel encodes MBF in mL/g/min). Subendocardial and subepicardial borders were contoured automatically using a machine learning approach. Where the LV outflow tract was included, or partial volume effect meant segments were too thin to contour, these segments were excluded from further analysis. Each segment was also further divided into subendocardial (inner 50%) and subepicardial (outer 50%) regions. Myocardial perfusion reserve (MPR) was calculated as stress MBF: rest MBF. The 16-segment American Heart Association (AHA) model[22] used for further segmentation of maximal wall thickness, LGE, T1, and perfusion maps.

cDTI data analysis

Data processing for segmental cDTI analysis was performed using MATLAB software (MathWorks, MA, USA). Quality control was undertaken by visual assessment with DW images corrupted by

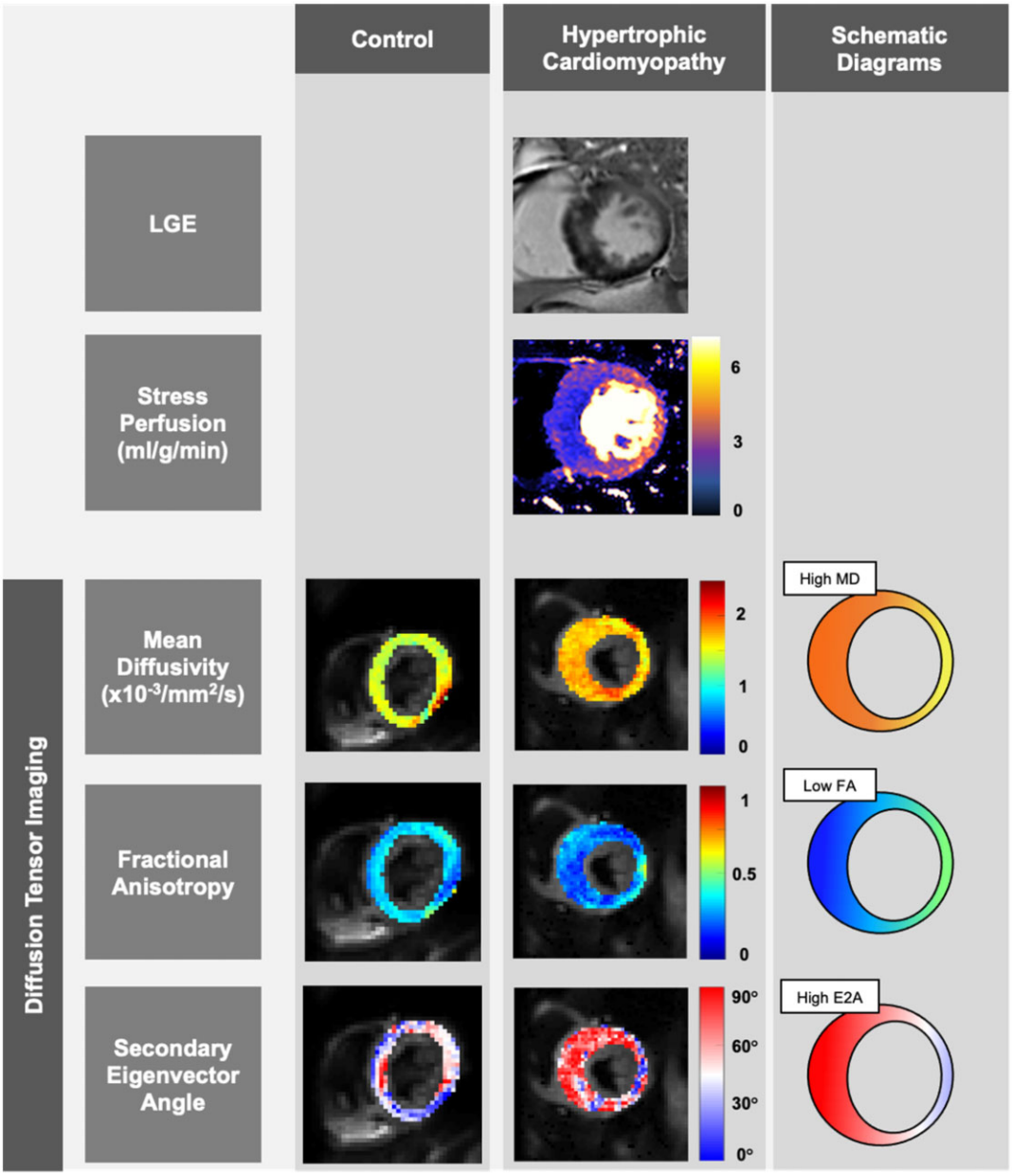

Figure 2 Representative maps for a healthy control subject and a patient with hypertrophic cardiomyopathy. Representative mid left ventricular slices obtained in a healthy control subject (first column) and a patient with hypertrophic cardiomyopathy (HCM) (second column), with schematic diagrams (third column). On the late gadolinium enhancement (LGE) image, there is evidence of midwall fibrosis in the hypertrophied septal segments, which corresponds with reduced myocardial blood flow on the stress perfusion maps. On the diffusion tensor imaging maps, in comparison to the control subject, the HCM patient has increased mean diffusivity, reduced fractional anisotropy, and increased secondary eigenvector angle values globally, even in segments with normal wall thickness and no scar.

artefact or failed registration omitted from further processing. Averaged magnitude images were generated from the registered data by averaging across repetitions, and diffusion tensors were calculated. Myocardial contours were drawn directly on the cDTI maps: in order to separate myocardial tissue from blood pool and minimize the effects of partial voluming, a conservative approach was adopted, ensuring the borders were drawn within the myocardial wall; cine-images were used as a visual guide. Tensor eigenvalues, MD, FA, and absolute E2A maps were assessed both globally and on a segmental basis. In order to investigate possible explanations for the subendocardial pattern of MVD seen in HCM, each segment of MD and FA maps were further divided into subendocardial (inner 50%) and subepicardial (outer 50%) regions. After data rejection, the number of repetitions for $b = 100\,s/mm^2$ were 11.6 ± 1.0, and for $b = 450\,s/mm^2$, 5.57 ± 0.96, respectively (inclusive of base and mid slices only; apical data was excluded from the study due to persistent data quality issues from unsuppressed fat, signal loss, and suboptimal signal-to-noise ratio).

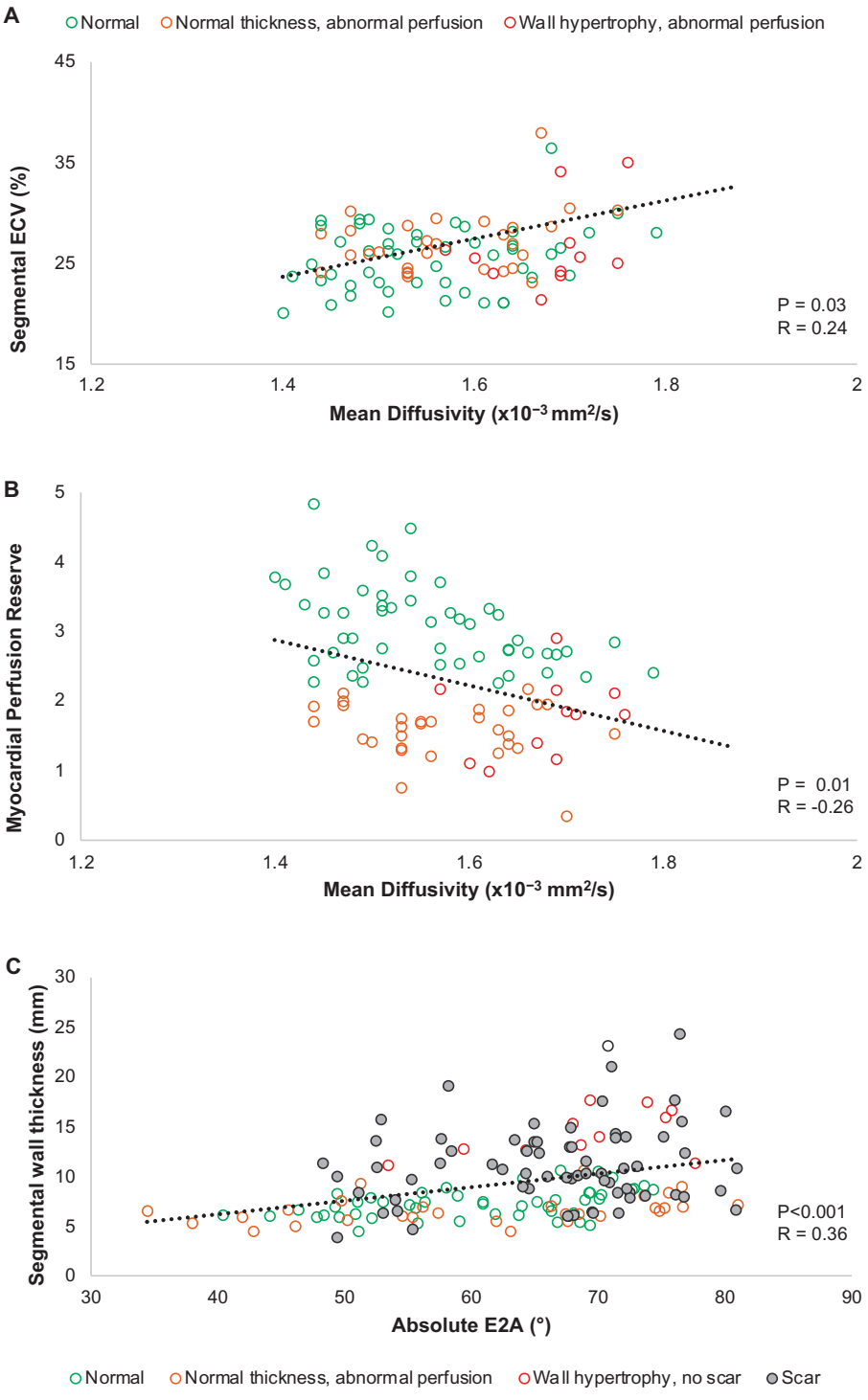

Figure 3 Correlations between segmental MD/ECV, MD/MPR, and absolute E2A/wall thickness. Even in the absence of scar, a positive correlation was noted between mean diffusivity (MD) and extracellular volume (ECV) in the segments of HCM patients (*A*). Segmental MD also correlated with myocardial perfusion reserve in corresponding non-scarred segments (*B*). Segmental absolute secondary eigenvector (E2A) in systole correlated with the wall thickness of corresponding segments in end-diastole.

Subgroup analysis

Subgroup analysis was carried out in order to investigate the cDTI characteristic of HCM segments with different morphological features (i.e. wall hypertrophy, abnormal perfusion and presence of scar). The normal range for myocardial blood flow at stress, rest and the perfusion reserve were derived from age- and sex-matched volunteers who underwent

Table 2 Results from subgroup analysis of HCM patients and healthy controls

Subgroups of segments	Controls	Group 1	Group 2	Group 3	Group 4	*P*-value
		'Normal'	'Normal wall thickness, abnormal perfusion'	'Abnormal wall thickness, abnormal perfusion'	'Scar'	
Variable cut-offs		Thickness ≤11 mm MPR ≥2.2 No LGE	Thickness ≤11 mm MPR <2.2 No LGE	Thickness >11 mm MPR <2.2 No LGE	LGE present	
Number of segments (%)	160 (100)[a]	63 (29)	45 (21)	22 (10)	86 (40)	
Wall thickness (mm)	7.6 ± 2.1[a]	7.8 ± 1.5	8.1 ± 1.6	12.1 ± 2.7	11.3 ± 4.3	<0.001
LGE (%)					12.0 ± 13.2	
Native T1 (ms)		1280 ± 13	1325 ± 14	1353 ± 26	1355 ± 56	<0.001
ECV (%)		25.5 ± 1.8	26.8 ± 1.8	25.4 ± 4.1	30.0 ± 2.7	<0.001
Stress MBF (mL/g/min)	2.5 ± 0.6[b]	1.72 ± 0.08	1.30 ± 0.09	1.27 ± 0.10	1.19 ± 0.08	<0.001
Rest MBF (mL/g/min)	0.6 ± 0.1[b]	0.66 ± 0.05	0.73 ± 0.05	0.69 ± 0.05	0.68 ± 0.04	0.324
MPR	4.0 ± 0.9[b]	2.77 ± 0.11	1.81 ± 0.11	1.94 ± 0.14	1.83 ± 0.10	<0.001
MD ($\times 10^{-3}$mm^2/s)	1.46 ± 0.07[a]	1.61 ± 0.09	1.59 ± 0.08	1.65 ± 0.06	1.67 ± 0.09	<0.001
FA	0.35 ± 0.02[a]	0.29 ± 0.04	0.28 ± 0.04	0.28 ± 0.02	0.26 ± 0.04	0.019
Absolute E2A (°)	38 ± 12[a]	60 ± 9	61 ± 6	69 ± 7	66 ± 6	<0.001

E2A, secondary eigenvector angle; ECV, extracellular volume; FA, fractional anisotropy; LGE, late gadolinium enhancement; MBF, mean blood flow; MD, mean diffusivity; MPR, myocardial perfusion reserve; MPR, myocardial perfusion reserved.
[a]Derived from 10 controls recruited in this study.
[b]Derived from 20 controls as per reference.[23]

perfusion imaging as previously reported[23] and were as follows: stress MBF 1.3–3.7 mL/g/min, rest MBF 0.4–1.8 mL/g/min, and MPR 2.2–5.8. Hence 2.2 was used as a cut-off to define segments with abnormal perfusion. All myocardial segments of HCM patients were subsequently classified into the following four subgroups: *Group 1* (titled 'normal') included segments with normal wall thickness (≤11 mm), normal perfusion reserve (≥2.2), and no visual LGE; *Group 2* (titled 'normal thickness, abnormal perfusion') included segments with normal wall thickness (≤11 mm), abnormal perfusion reserve (<2.2), and no visual LGE; *Group 3* (titled 'wall hypertrophy, abnormal perfusion') included segments with abnormal wall thickness (>11 mm), abnormal perfusion reserve (<2.2) and no visual LGE; and *Group 4* (titled 'scar') included all segments with visual evidence of LGE.

Statistical analysis

Statistical analysis was performed using the commercially available software, Statistical Package for the Social Sciences (SPSS) Statistics 22.0 (IBM Corporation, Armonk, NY, USA). Normality was assessed through the Shapiro–Wilk test and variance was assessed by the Levene's test for equality of variance. Continuous variables are reported as mean ± standard deviation. When comparing HCM with healthy volunteers, normally distributed data were compared using Student's *t*-test, non-normally distributed data by the Kruskal–Wallis test and categorical data were compared using χ^2 tests. For subgroup and regional comparisons of CMR parameters between the different groups of HCM segments, to account for within-subject measurements, a linear mixed effects model was used; *post hoc* pairwise testing with Bonferroni correction was used to detect significant differences between subgroups. Pearson correlation analysis was used to calculate the correlations between independent variables. Statistical tests were two-tailed and a *P*-value of ≤0.05 was considered to be statistically significant.

Results

The study flowchart is shown in *Figure 1*. Twenty HCM patients (M:F = 8:12, aged 48 ± 18 years) were included in the study; baseline characteristics are shown in *Table 1*. Five of the HCM patients were gene-positive (MYH7 × 3, TNNI3 × 1, MYBPC3 × 1). The vast majority (18/20) had septal hypertrophy, while 2 HCM subjects had LV hypertrophy (LVH) confined to anterior and anterolateral walls. Two patients were unable to tolerate the side-effects of adenosine, hence the stress perfusion sequence was omitted. HCM patients had a mean ejection fraction of 67 ± 6%, mean myocardial mass of 149 ± 80 g, and mean LGE of 5.9 ± 10.1%. Ten normal controls (M:F = 4:6, aged 27 ± 9 years) underwent cDTI. Of all basal and mid slice segments, 31/240 segments (13%) were rejected due to imaging artefacts that remained post data rejection; these image artefacts resulted from unsuppressed fat, localized signal loss, or low signal–noise ratio.

Representative LGE, perfusion and cDTI maps are shown in *Figure 2*. HCM patients had significantly increased global MD (MD_{HCM} 1.62 ± 0.10 × 10^{-3} mm^2/s vs. $MD_{Controls}$ 1.47 ± 0.1 × 10^{-3} mm^2/s, $P < 0.001$), absolute E2A ($E2A_{HCM}$ 64 ± 10° vs. $E2A_{Controls}$ 36 ± 12°, $P < 0.001$), and significantly lower FA (FA_{HCM} 0.29 ± 0.04 vs. $FA_{Controls}$ 0.34 ± 0.04, $P < 0.001$) than controls. HCM patients had significantly lower myocardial blood flow at both stress and at rest, and significantly lower mean MPR than controls (stress MBF_{HCM} = 1.4 ± 0.5 mL/g/min, stress $MBF_{Controls}$ = 2.5 ± 0.6 mL/g/min, $P < 0.001$, MPR_{HCM} = 2.1 ± 0.8, $MPR_{Controls}$ = 4.0 ± 0.9, $P < 0.001$). MD and ECV are known to increase in areas of scarring and fibrosis. Even in non-scarred segments, segmental MD correlated moderately with ECV ($P = 0.03$, *Figure 3A*) and MPR in the

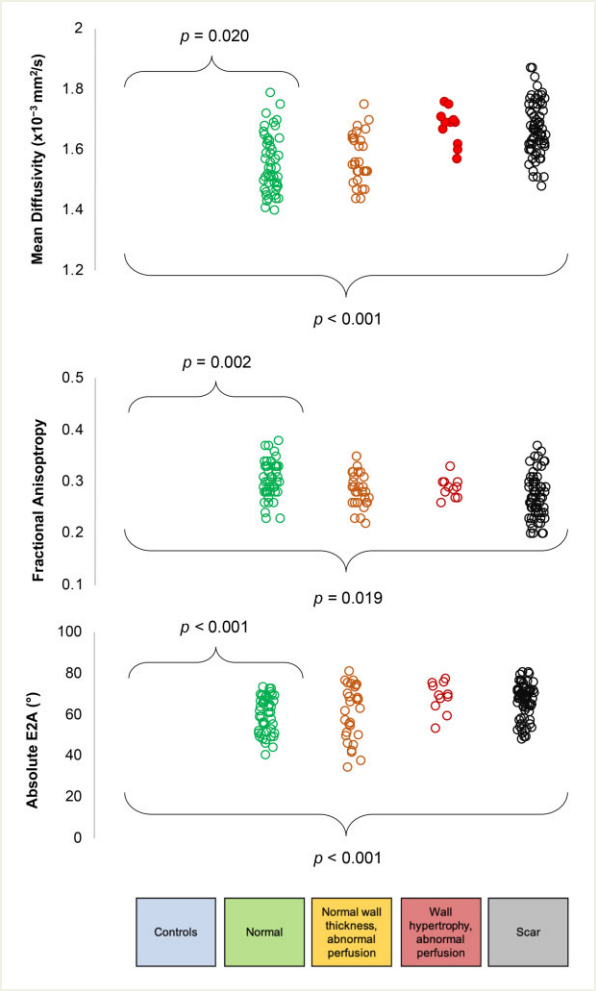

Figure 4 Subgroup analysis of cDTI parameters between different HCM segments. Segmental mean diffusivity (MD), fractional anisotropy (FA), and absolute secondary eigenvector angle (E2A) values are plotted according to the classification of the segments. 'Normal' HCM segments had significantly increased MD, absolute E2A, and decreased FA than controls.

corresponding segment ($P = 0.01$, *Figure 3B*), while segmental absolute E2A correlated moderately with wall thickness ($P < 0.001$, *Figure 3C*) across all segments. HCM patients had higher global T1 than the departmental 3.0T scanner reference range (1323 ± 75 vs. 1158 ± 80 ms).

Subgroup analyses

The results of subgroup analysis are displayed in *Table 2* and *Figure 4*. Of the 216 analysed segments, 63 (29%) were classified as 'normal' (Group 1), 45 (21%) had 'normal thickness, abnormal perfusion' (Group 2), 22 (10%) had 'wall hypertrophy, abnormal perfusion' (Group 3), and 86 (40%) had 'scar' (Group 4). Of note, there were no hypertrophied segments with normal perfusion. Compared to controls, 'normal' (Group 1) HCM segments had significantly increased MD ($MD_{HCM\ Group\ 1:\ normal}$ $1.61 \pm 0.09 \times 10^{-3}$ mm^2/s vs. $MD_{Controls}$ $1.46 \pm 0.07 \times 10^{-3}$ mm^2/s, $P = 0.02$), increased absolute E2A ($E2A_{HCM\ Group\ 1:\ normal}$ 60 ± 9° vs. $E2A_{Controls}$ 38 ± 12°, $P < 0.001$), and decreased FA ($FA_{Group\ 1:\ normal}$ = 0.29 ± 0.04 vs. $FA_{Controls}$ = 0.35 ± 0.02, $P = 0.002$). Out of the normal segments, 81% were located not in the septum: there was no significant difference in MD, FA, or E2A between septal and non-septal normal segments.

Compared to the other groups, segments with LGE (Group 4) had significantly higher MD ($MD_{HCM\ scar}$ $1.67 \pm 0.09 \times 10^{-3}$ mm^2/s vs. $MD_{HCM\ Groups\ 1–3:\ no\ scar}$ $1.58 \pm 0.09 \times 10^{-3}$ mm^2/s, $P = 0.001$) and significantly lower FA ($FA_{HCM\ Group\ 4:\ scar}$ 0.26 ± 0.04 vs. $FA_{HCM\ Groups\ 1–3:\ no\ scar}$ 0.30 ± 0.03 $P = 0.04$). Of note, there was no significant difference in absolute E2A between hypertrophied segments with and without scar. Hypertrophied segments (Groups 3 and 4) had significantly higher E2A than non-hypertrophied segments (67 ± 7° vs. 61 ± 10°, $P = 0.016$).

Regional variance in perfusion and cDTI

In HCM patients, subendocardial MBF during stress was significantly lower than subepicardial MBF during stress (1.28 ± 0.65 mL/g/min vs. 1.47 ± 0.56 mL/g/min, $P = 0.001$) and subendocardial MPR was significantly lower than subepicardial MPR (1.85 ± 0.83 vs. 2.28 ± 0.87, $P < 0.001$). Among controls, there was no difference between subendocardial and subepicardial MD, however HCM patients had significantly higher subendocardial MD than subepicardial MD (MD_{endo} $1.61 \pm 0.08 \times 10^{-3}$ mm^2/s vs. MD_{epi} $1.56 \pm 0.18 \times 10^{-3}$ mm^2/s, $P = 0.003$) as shown in *Figure 5*. All HCM segments were then subdivided into segments with normal perfusion reserve (MPR ≥ 2.2) and abnormal perfusion reserve (MPR < 2.2). Even segments with normal perfusion reserve had significantly higher subendocardial MD than subepicardial MD (MD_{endo} $1.63 \pm 0.10 \times 10^{-3}$ mm^2/s vs. MD_{epi} $1.57 \pm 0.11 \times 10^{-3}$ mm^2/s, $P = 0.035$). This pattern was also seen in segments with abnormal perfusion reserve (MD_{endo} $1.62 \pm 0.14 \times 10^{-3}$ mm^2/s vs. MD_{epi} $1.56 \pm 0.12 \times 10^{-3}$ mm^2/s, $P = 0.003$). Subendocardial FA and subepicardial FA did not vary significantly in controls (FA_{endo} 0.34 ± 0.05 vs. FA_{epi} 0.34 ± 0.05, $P = 0.82$) or HCM patients (FA_{endo} 0.28 ± 0.06 vs. FA_{epi} 0.29 ± 0.06, $P = 0.50$).

Discussion

In clinical practice, recognizing the phenotypic expression of HCM is largely limited to the detection of wall hypertrophy and scar formation. This approach fails to acknowledge several of the underlying pathophysiological changes, such as MVD that is thought to precede macroscopic change and yet affect long-term clinical outcome.[5,24] In this prospective study, we compare 20 HCM patients with controls, use quantitative perfusion to differentiate segments with normal and abnormal perfusion reserve; and use cDTI to gain insights into underlying microstructural differences. The main findings from our study include: (i) HCM patients had increased MD, increased absolute E2A and reduced FA compared to controls, even in segments with normal thickness and normal perfusion reserve; (ii) subendocardial MD was significantly higher than subepicardial MD, matching the pattern seen with perfusion imaging. The results from this study could help elucidate some early pathophysiological changes that occur in patients with HCM.

In agreement with the largest quantitative perfusion study of HCM patients to date,[24] our results demonstrate stress MBF and MPR to

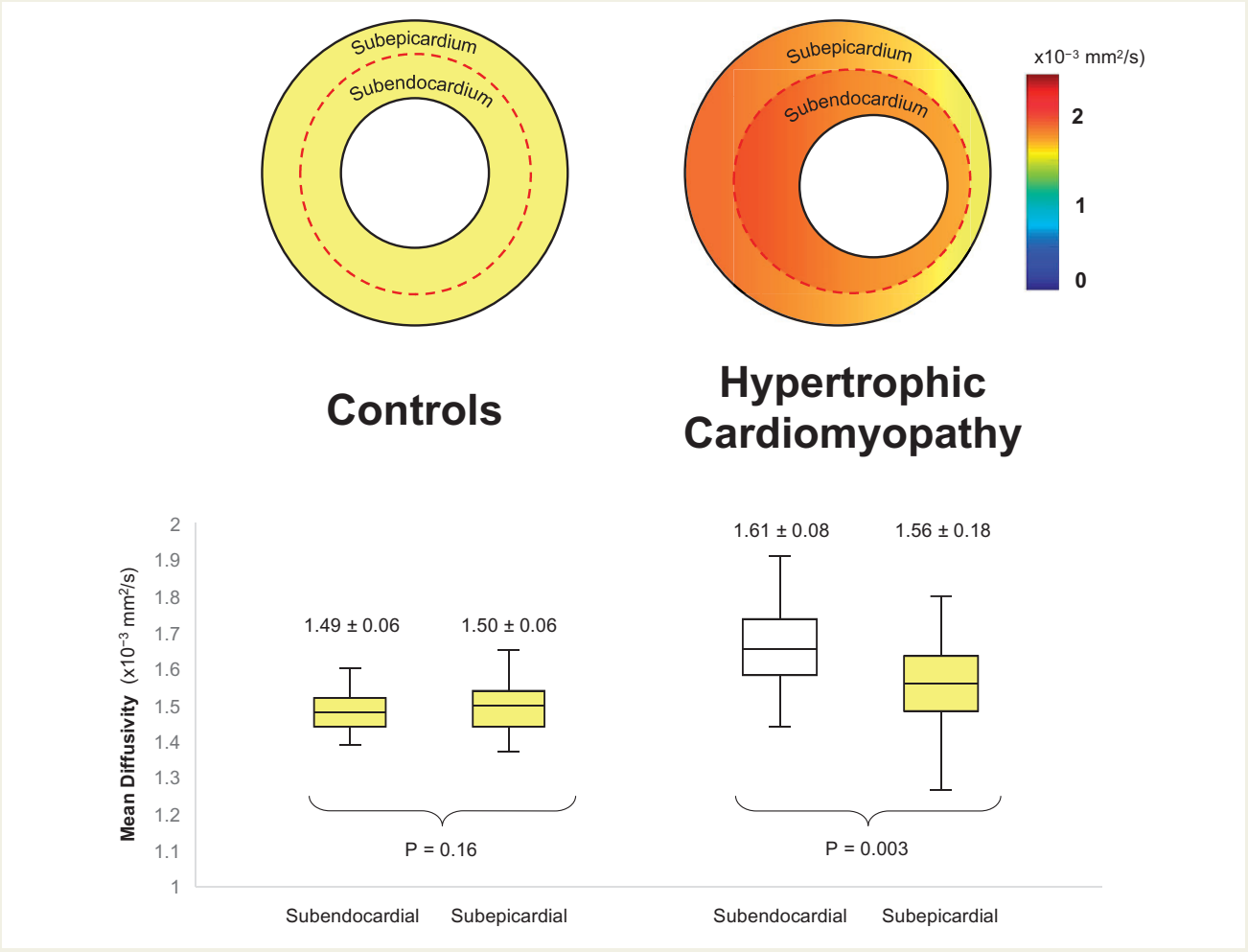

Figure 5 Regional MD in controls and HCM patients. In controls, there were no significant differences in subendocardial and subepicardial mean diffusivity (MD); however, in HCM patients, subendocardial MD was significantly higher than subepicardial MD.

be reduced, particularly at the subendocardium; this occurs not only in hypertrophied and scarred segments but also in segments that morphologically appear 'normal'. In fact, 42% of the segments with wall thickness <11 mm had abnormally low MPR (>2.5 SDs lower than control cohort range), while all 108 segments with wall thickness >11 mm had abnormally low MPR, supporting the hypothesis that MVD precedes the development of macroscopic abnormalities.[24,25]

Using cDTI, we compared the myocardium of controls with the myocardial segments of HCM patients that had normal wall thickness, normal perfusion reserve, and no scar, and still noted several distinct microstructural differences, suggesting such changes may also precede the development of macroscopic abnormalities. Firstly, in these 'normal' HCM segments, MD was significantly higher than controls, suggesting water molecules are able to diffuse more freely. In healthy specimens, cell membranes provide a bio-physiological barrier for diffusion; and previous authors have observed how areas with high MD correlate with areas of scarring, fibrosis, and increased ECV, where cellular apoptosis has resulted in the breakdown of cell membranes.[9,25] However in the 'normal' HCM segments in our study, ECV values were comparable with normal published values,[26] and there was no evidence of scar with LGE, warranting the exploration of alternative explanations. On a cellular level, a physical increase in myocyte size is a hallmark of HCM.[2] As previously shown in brain studies using DW imaging,[27,28] an increase in intracellular volume creates a greater distance between restrictive cell membranes, which results in increase in MD. Hence the increased subendocardial MD could be representative of regional myocyte hypertrophy. Various histological studies have demonstrated subendocardial arterioles in HCM patients to have smaller cross-sectional lumen area[29] and greater coronary flow resistance[30] than controls, and authors have speculated whether this could be due to compressive effects of regional hypertrophy.[31,32] This hypothesis is supported by our finding of an inverse correlation between subendocardial MD and MPR, however histological corroboration of this is still lacking. The incremental increase in MD in segments with hypertrophy and scarring in our cohort correlates with an increase in ECV and LGE; and would seem to be more attributable to a gradual interstitial fibrotic process that ensues in these segments, as other authors have observed.[9,25]

In a recent pre-clinical cDTI study in which rat hearts underwent pressure-overload LVH, the authors noted regional structural remodelling in the form of increased dispersion of the HA, most notably at the subendocardium of the specimens.[33] They did not report a subendocardial rise in MD; however, it is worth noting that the pathophysiology of LVH in HCM is driven by sarcomeric mutations rather than pressure-overload. In our results, we did not observe a significant correlation between segmental MD and wall thickness, and it remains unclear if myocyte hypertrophy directly equates with wall hypertrophy.

Previous studies have observed absolute E2A to be globally increased in HCM patients compared to controls suggesting that the myocardial sheetlets adopt hypercontracted configurations during systole[13,14,26]; however, in this study, we demonstrate this to be the case even in segments with normal thickness and normal perfusion. Previous authors have speculated whether the compressive deformation of intramyocardial blood vessels during systole can explain the increased coronary flow resistance in these patients[27]; however, results from our study are unable to corroborate this, as absolute E2A did not vary significantly between segments with normal and abnormal perfusion reserve. What we did note was a correlation between segmental absolute E2A and wall thickness, and E2A was significantly higher in hypertrophied segments (>11 mm) than non-hypertrophied segments. It is the dynamic rearrangement of the myocardial sheetlets that drives radial thickening during systole; however, in HCM patients, sheetlet mobility is impaired so they remain hypercontracted and fail to relax in diastole.[26] This could explain why segments with higher absolute E2A in systole had greater LV wall thickness in end-diastole.

FA reflects the anisotropy of diffusion; studies have shown FA to correlate inversely with histological measurements of collagen, a major component of fibrotic tissue.[11] This explains the significant reduction in FA in segments with scar in our study. Histological analysis of HCM patients undergoing surgical myomectomy has found that, in addition to collagen deposition, the specimens also had disorganized matrix connective tissue.[28] The diffusion of water molecules in enlarged cardiomyocytes within disorganized matrixes is more random and isotropic, leading to lower FA values.[10] Hence low FA in the absence of scar is suggestive of underlying cardiomyocyte disarray, which could explain why FA values were lower in HCM patients than controls even in segments with no scar. Preclinical studies on mice have noted cardiomyocyte disarray to be an early response to sarcomeric mutations, while hypertrophy and fibrosis occur later and are more secondary responses.[6] It remains to be seen if low FA values in the absence of scar in HCM patients can identify patients who are genotype-positive but phenotype-negative. A recent study by Ariga *et al.*[10] demonstrated an association between low FA and ventricular arrhythmia in HCM patients. The authors used an alternative stimulated echo cDTI sequence which involves longer diffusion times, hence direct comparison of values cannot be made with our results; however, the study still highlights the clinical relevance of low FA in the absence of scar in this population.

Limitations

The study sample is relatively small, but in keeping with similar studies.[14] cDTI volunteers were not age-matched to the HCM subjects; however, it is yet to be established whether DTI parameters change with age. The ECV, MPR, and LGE of healthy volunteers were not obtained, as it was not felt ethically justifiable to administer contrast in this cohort. Conclusions drawn from this study are based on correlations with published evidence and other cardiac MRI markers, whereas validation with histological specimens would be preferable. cDTI in a novel technique still under validation: as such the accuracy of DTI measurements in relation to the impact of partial volume effects requires further investigations on a large multicentre scale.

Conclusion

By using a combination of quantitative perfusion and cDTI, our results demonstrate a complex relationship between abnormal anatomy, abnormal physiology, and abnormal microstructure in HCM patients, the concomitant effects of which may help explain the underlying mechanisms behind MVD. Even in segments which lack phenotypic features of HCM, diffusion is more isotropic than controls, the myocardial sheetlets adopt hypercontracted configurations in mid-systole, and the MD is higher particularly in the subendocardium, indicating regional remodelling which may impact on MPR. These findings highlight some of the microstructural changes that may precede macroscopic abnormalities and could prove useful for early detection of the disease, family screening and early phenotyping. Further larger studies will be needed to validate these findings.

Acknowledgements

The authors thank the clinical staff of the CMR Department at Leeds General Infirmary and the research nurses of Leeds Institute of Cardiovascular and Metabolic Medicine, University of Leeds, for their assistance in recruiting, scanning, and collecting data for this study.

Funding

A.D. is a PhD student at the University of Leeds and is funded by Heart Research UK (RG2668/18/20). S.P. is funded by a British Heart Foundation Chair (CH/16/2/32089). L.R.L. is funded by Medical Research Council UK Clinical Academic Partnership (MR/T005181/1). E.D.A. acknowledges funding from British Heart Foundation Intermediate Clinical Research Fellowship (FS/13/71/30378). The authors have reported that they have no relationships relevant to the contents of this paper to disclose.

Conflict of interest: none declared.

References

1. Maron BJ, Maron MS. Hypertrophic cardiomyopathy. *Lancet* 2013;**381**:242–55.
2. Harvey PA, Leinwand LA. The cell biology of disease: cellular mechanisms of cardiomyopathy. *J Cell Biol* 2011;**194**:355–65.
3. Bravo PE. Is there a role for cardiac positron emission tomography in hypertrophic cardiomyopathy? *J Nucl Cardiol* 2019;**26**:1125–34.
4. Maron MS, Olivotto I, Maron BJ, Prasad SK, Cecchi F, Udelson JE *et al.* The case for myocardial ischemia in hypertrophic cardiomyopathy. *J Am Coll Cardiol* 2009;**54**:866–75.
5. Cecchi F, Olivotto I, Gistri R, Lorenzoni R, Chiriatti G, Camici PG. Coronary microvascular dysfunction and prognosis in hypertrophic cardiomyopathy. *N Engl J Med* 2003;**349**:1027–35.
6. Varnava AM, Elliott PM, Sharma S, Mckenna J, Davies MJ. Hypertrophic cardiomyopathy: the interrelation of disarray, fibrosis, and small vessel disease. *Heart* 2000;**84**:476–82.
7. Basser PJ. Inferring microstructural features and the physiological state of tissues from diffusion-weighted images. *NMR Biomed* 1995;**8**:333–44.
8. Basser PJ, Mattiello J, LeBihan D. MR diffusion tensor spectroscopy and imaging. *Biophys J* 1994;**66**:259–67.

9. Wu R, An DA, Shi RY, Hua CB, Jiang M, Bacyinski A *et al.* Myocardial fibrosis evaluated by diffusion-weighted imaging and its relationship to 3D contractile function in patients with hypertrophic cardiomyopathy. *J Magn Reson Imaging* 2018;**48**:1139–46.
10. Ariga R, Tunnicliffe EM, Manohar SG, Mahmod M, Raman B, Piechnik SK *et al.* Identification of myocardial disarray in patients with hypertrophic cardiomyopathy and ventricular arrhythmias. *J Am Coll Cardiol* 2019;**73**:2493–502.
11. Abdullah OM, Drakos SG, Diakos NA, Wever-Pinzon O, Kfoury AG, Stehlik J *et al.* Characterization of diffuse fibrosis in the failing human heart via diffusion tensor imaging and quantitative histological validation NIH public access. *NMR Biomed* 2014;**27**:1378–86.
12. Teh I, McClymont D, Burton RAB, Maguire ML, Whittington HJ, Lygate CA *et al.* Resolving fine cardiac structures in rats with high-resolution diffusion tensor imaging. *Sci Rep* 2016;**6**:30573.
13. Nielles-Vallespin S, Khalique Z, Ferreira PF, de Silva R, Scott AD, Kilner P *et al.* Assessment of myocardial microstructural dynamics by *in vivo* diffusion tensor cardiac magnetic resonance. *J Am Coll Cardiol* 2017;**69**:66.
14. Das A, Chowdhary A, Kelly C, Teh I, Stoeck CT, Kozerke S *et al.* Insight into myocardial microstructure of athletes and hypertrophic cardiomyopathy patients using diffusion tensor imaging. *J Magn Reson Imaging* 2021;**53**: 73–82.
15. Elliott PM. 2014 ESC guidelines on diagnosis and management of hypertrophic cardiomyopathy. *Russ J Cardiol* 2015;**72**:1054–1126.
16. Kellman P, Hansen MS, Nielles-Vallespin S, Nickander J, Themudo R, Ugander M *et al.* Myocardial perfusion cardiovascular magnetic resonance: optimized dual sequence and reconstruction for quantification. *J Cardiovasc Magn Reson* 2017;**19**: 43.
17. Kramer CM, Barkhausen J, Flamm SD, Kim RJ, Nagel E; Society for Cardiovascular Magnetic Resonance Board of Trustees Task Force on Standardized Protocols. Standardized cardiovascular magnetic resonance (CMR) protocols 2013 update. *J Cardiovasc Magn Reson* 2013;**15**:91.
18. Nguyen C, Fan Z, Sharif B, He Y, Dharmakumar R, Berman DS *et al. In vivo* three-dimensional high resolution cardiac diffusion-weighted MRI: a motion compensated diffusion-prepared balanced steady-state free precession approach. *Magn Reson Med* 2014;**72**:1257–67.
19. Nguyen CT, Christodoulou AG, Coll-Font J, Ma S, Xie Y, Reese TG *et al.* Free-breathing diffusion tensor MRI of the whole left ventricle using second-order motion compensation and multitasking respiratory motion correction. *Magn Reson Med* 2021;**85**:2634–48.
20. Augusto JB, Davies RH, Bhuva AN, Knott KD, Seraphim A, Alfarih M *et al.* Diagnosis and risk stratification in hypertrophic cardiomyopathy using machine learning wall thickness measurement: a comparison with human test-retest performance. 2021;3: e20–8.
21. Freitas P, Ferreira AM, Arteaga-Fernández E, De Oliveira Antunes M, Mesquita J, Abecasis J *et al.* The amount of late gadolinium enhancement outperforms current guideline-recommended criteria in the identification of patients with hypertrophic cardiomyopathy at risk of sudden cardiac death. *J Cardiovasc Magn Reson* 2019;**21**:50.
22. Cerqueira MD, Weissman NJ, Dilsizian V, Jacobs AK, Kaul S, Laskey WK *et al.* Standardized myocardial segmentation and nomenclature for tomographic imaging of the heart: a statement for healthcare professionals from the Cardiac Imaging Committee of the Council on Clinical Cardiology of the American Heart Association. *J Nucl Cardiol* 2002;**9**:240–5.
23. Brown LAE, Onciul SC, Broadbent DA, Johnson K, Fent GJ, Foley JRJ *et al.* Fully automated, inline quantification of myocardial blood flow with cardiovascular magnetic resonance: repeatability of measurements in healthy subjects. *J Cardiovasc Magn Reson* 2018;**20**:48.
24. Camaioni C, Knott KD, Augusto JB, Seraphim A, Rosmini S, Ricci F *et al.* Inline perfusion mapping provides insights into the disease mechanism in hypertrophic cardiomyopathy. *Heart* 2020;**106**:824–9.
25. Petersen SE, Jerosch-Herold M, Hudsmith LE, Robson MD, Francis JM, Doll HA *et al.* Evidence for microvascular dysfunction in hypertrophic cardiomyopathy. *Circulation* 2007;**115**:2418–25.
26. Ferreira PF, Kilner PJ, Mcgill LA, Nielles-Vallespin S, Scott AD, Ho SY *et al. In vivo* cardiovascular magnetic resonance diffusion tensor imaging shows evidence of abnormal myocardial laminar orientations and mobility in hypertrophic cardiomyopathy. *J Cardiovasc Magn Reson* 2014;**16**:87.
27. Raphael CE, Cooper R, Parker KH, Collinson J, Vassiliou V, Pennell DJ *et al.* Mechanisms of myocardial ischemia in hypertrophic cardiomyopathy insights from wave intensity analysis and magnetic resonance. *J Am Coll Cardiol* 2016;**68**: 1651–60.
28. Wigle ED, Sole MJ, Williams WC. Pathologic fibrosis and matrix connective tissue in the subaortic myocardium of patients with hypertrophic cardiomyopathy. *J Am Coll Cardiol* 1991;**17**:1343–51.
29. Schwartzkopff B, Mundhenke M, Strauer BE.Alterations of the Architecture of Subendocardial Arterioles in Patients With Hypertrophic Cardiomyopathy and Impaired Coronary Vasodilator Reserve: A Possible Cause for Myocardial Ischemia 11This study was supported by Grant SFB 242: Koronare Herzkrankheit: Prävention und Therapie akuter Komplikationen from the Deutsche Forschungsgemeinschaft, Bonn, Germany. Journal of the American College of Cardiology 1998;**31**:1089–96.
30. Krams R, Kofflard MJM, Duncker DJ, Von Birgelen C, Carlier S, Kliffen M *et al.*. Decreased Coronary Flow Reserve in Hypertrophic Cardiomyopathy Is Related to Remodeling of the Coronary Microcirculation. Circulation 1998;**97**:230–3.
31. Marszalek RJ, John Solaro R, Wolska BM.Coronary arterial vasculature in the pathophysiology of hypertrophic cardiomyopathy. Pflugers Arch 2019;**471**: 769–80.
32. Antunes MdO, Scudeler TL.Hypertrophic cardiomyopathy. Int J Cardiol Heart Vasc 2020;**27**:100503.